A chemo-enzymatic pathway to expand cellooligosaccharide chemical space through amine bond introduction

Awilda Maccow, Hanna Kulyk, Etienne Severac, Sandrine Morel, Claire Moulis, Guillaume Boissonnat, Magali Remaud-Simeon, David Guieysse

Title:

A chemo-enzymatic pathway to expand cellooligosaccharide chemical space through amine bond introduction

Author names:

Awilda Maccow [a], Hanna Kulyk [a,c], Etienne Severac [a], Sandrine Morel [a], Claire Moulis [a], Guillaume Boissonnat [b], Magali Remaud-Simeon*[a] and David Guieysse *[a]

Affiliations:

[a] Biotechnology Institute (TBI), Université de Toulouse, CNRS, INRAE, INSA, 135 Avenue de Rangueil, CEDEX 04, F-31077 Toulouse, France.

[b] PILI, 226 rue Saint Denis, 75002 Paris.

[c] MetaboHUB-MetaToul, National Infrastructure of Metabolomics and Fluxomics, France.

E-mail address:

Awilda Maccow: awilda.maccow@hotmail.fr

Hanna Kulyk: hbarbier@insa-toulouse.fr

Etienne Severac: e_severa@insa-toulouse.fr

Sandrine Morel : sandrine.morel@insa-toulouse.fr

Claire Moulis : claire.moulis@insa-toulouse.fr

Guillaume Boissonnat : guillaume.boissonnat@pili.bio

Magali Remaud-Simeon : remaud@insa-toulouse.fr

David Guieysse: guieysse@insa-toulouse.fr

Correspondence to: David Guieysse (guieysse@insa-toulouse.fr) at Biotechnology Institute (TBI), Université de Toulouse, CNRS, INRAE, INSA, 135 Avenue de Rangueil, CEDEX 04, F-31077 Toulouse, France

* Corresponding author

Abstract:

Enzymatic functionalization of oligosaccharides is a useful and environmentally friendly way to expand their structural chemical space and access to a wider range of applications in the health, food, feed, cosmetics and other sectors. In this work, we first tested the laccase/TEMPO system to generate oxidized forms of cellobiose and methyl β-D-cellobiose, and obtained high yields of novel anionic disaccharides (>60 %) at pH 6.0. Laccase/TEMPO system was then applied to a mix of cellooligosaccharides and to pure D-cellopentaose. The occurence of carbonyl and carboxyl groups in the oxidation products was shown by LC-HRMS, MALDI-TOF and reductive amination of the carbonyl groups was attempted with *p*-toluidine a low molar mass amine to form the Schiff base, then reduced by 2-picoline borane to generate a more stable amine bond. The new grafted products were characterized by LC-HRMS, LC-UV-MS/MS and covalent grafting was evidenced. Next, the same procedure was adopted to successfully graft a dye, the rhodamine 123, larger in size than toluidine. This two-step chemo-enzymatic approach, never reported before, for functionalization of oligosaccharides, offers attractive opportunities to anionic cellooligosaccharides and derived glucoconjugates of interest for biomedical or neutraceutical applications. It also paves the way for more environmentally-friendly cellulose fabric staining procedures.

Keywords:

Cellooligosaccharides; Laccase, Oxidation; Reductive amination; Amino-chromophores

Abbreviations:

LMS, Laccase Mediated System; TvL, *Trametes versicolor* laccase; COS, cellooligosaccharides; MOS, maltooligosaccharides; pic-BH_3, 2-picoline borane; *p*-T, *p*-toluidine; RHO123, rhodamine 123; TEMPO, 2,2,6,6-Tetramethyl-1-piperidinyloxy; Glc2, cellobiose; me-β-Glc2, methyl β-D-cellobiose; D-cellopentaose, Glc5;

1. Introduction

Functional oligosaccharides are biomolecules that are increasingly in demand in the food, feed, cosmetics, healthcare or agrochemical sectors due to their wide range of applications as food ingredients, non-digestible prebiotic supplements, bulking agents, drug carriers, immunostimulators, antioxidant, anti-inflammatory and more. (Catenza & Donkor, 2021; Ibrahim, 2018; Logtenberg et al., 2021; Mano et al., 2018; Patel & Goyal, 2011). The most common oligosaccharides (fructo-, galacto-, xylo-, gluco-, or manno-oligosaccharides) are homogeneous and neutral. However, oligosaccharide diversity also covers heterogenous and even charged structures such as those found in pectin, alginate or carrageenan (Guo et al., 2022; Liu, Liu, Zhang, Yi, & Everaert, 2021; Vasudevan, Lee, & Lee, 2021). Furthermore, oligosaccharide conjugation can be used to generate structures with unique physico-chemical or biological properties that offer numerous advantages for designing biological probes, carbohydrate-based vaccines, drug delivery agents, etc. (Astronomo & Burton, 2010; Humpierre et al., 2022; Kay, Cuccui, & Wren, 2019).

Among oligosaccharides, cellooligosaccharides (COS) composed of β-1,4 linked glucosyl units are gaining attention for their functional properties, which are of interest to the food, feed and cosmetics industries (Cangiano, Yohe, Steele, & Renaud, 2020; Jiao et al., 2014; Uyeno, Shigemori, & Shimosato, 2015; Yamasaki, Ibuki, Yaginuma, & Tamura, 2013; Zhong, Ukowitz, Domig, & Nidetzky, 2020). They can be produced by controlled chemical or enzymatic hydrolysis of cellulose or using non-thermal technologies such as ultrasound (Billès, Coma, Peruch, & Grelier, 2017; Jérôme, Chatel, & De Oliveira Vigier, 2016). Alternatively, enzyme-based synthetic cascades involving sucrose, cellobiose and cellodextrin phosphorylases have also been proposed. Cell-free or whole cell processes have proven efficient, achieving high production yields with good oligosaccharide size control (Schwaiger, Voit, Wiltschi, & Nidetzky, 2022; Zhong et al., 2020). Surprisingly, the oxidation of COS with oxidases has been little studied to access a wider panel of ionic structures. Using a glucooligosaccharide oxidase, the C1 carbonyl group at the reducing end of COS was efficiently converted to a carboxyl group (Vuong et al., 2013). Recently, COS-based glycoconjugates were also obtained by oxidizing COS with a C4-specific lytic polysaccharide monooxygenase to generate a ketone group at the C-4 position of the non-reducing end of the oxidation product, which then reacted spontaneously with an amino group of 2-(aminooxy)-1-ethanaminium dichloride (Westereng et al., 2020). COS oxidation with laccase (EC 1.10.3.2, benzenediol:oxygen reductases) or using TEMPO chemistry has never been described.

Laccases are polyphenol-oxidases belonging to the blue multicopper oxidase family (Morozova, Shumakovich, Shleev, & Yaropolov, 2007; Solomon, Sundaram, & Machonkin, 1996; Yoshida, 1883).

They catalyze the reduction of dioxygen to water concomitantly with the oxidation of a substrate, typically a phenolic compound of lignin (Mate & Alcalde, 2017). They are also finding a growing number of applications in organic chemistry, soil and water bioremediation, and biofuel production (Arregui et al., 2019; Mate & Alcalde, 2017; Theerachat, Guieysse, Morel, Remaud-Simeon, & Chulalaksananukul, 2019). Fungal laccases are particularly interesting because of their high redox potential (Baldrian, 2006). When the size of the substrate or its redox potential are too high, mediators can be used in the so called "Laccase Mediator System" (LMS) (d'Acunzo, Galli, Gentili, & Sergi, 2006). Marzorati et al. (2005) first reported the oxidation of methyl glucoside, methyl galactoside, methyl mannoside, trehalose and amygdalin with *Trametes pubescens* laccase and TEMPO (2,2,6,6-tetramethylpiperidine-1-oxyl) as mediator and showed the selective oxidation of the C-6 hydroxyl group to the corresponding carboxyl group (Marzorati, Danieli, Haltrich, & Riva, 2005). Similar results were obtained with alkyl glycosides (octyl β-glucoside, dodecyl maltoside and hexadecyl maltoside) using the laccase from *Trametes versicolor* (Ngo, Grey, & Adlercreutz, 2020a, b). In addition, cleavage of the α-1,4-osidic bond of maltoside could be detected, as well as traces of C=C double bond or keto groups at C-3, C-2 or C-4 position of the sugar rings (Ngo et al., 2020a). LMS also served to synthesize glycoconjugates by oxidizing the primary hydroxyl groups of oligosaccharides to carbonyl groups that reacted spontaneously with aminated molecules to form a Schiff base (-CH=N-). This approach was applied to the grafting of tyrosine onto β-cyclodextrin (Yu, Wang, Yuan, Fan, & Wang, 2016). LMS using TEMPO also enabled oxidation of cellulosic pulp and cellulose nanofibers by introducing carbonyl and/or carboxyl groups but was never applied to cellooligosaccharides (Jaušovec, Vogrinčič, & Kokol, 2015; Jiang et al., 2017; Jiang et al., 2021; Patel, Ludwig, Haltrich, Rosenau, & Potthast, 2011; Quintana, Roncero, Vidal, & Valls, 2017).

In the present study, we tested for the first time the efficiency of the LMS system to oxidize D-cellobiose (Glc2), methyl β-D-cellobiose (me-β-Glc2), a mixture of COS and D-cellopentaose (Glc5) to generate anionic COS as well as cello-conjugates. The oxidation products were characterized in detail using $^{1}H/^{13}C$ NMR, LC-HRMS and LC-HRMS/MS. We demonstrated the presence of carbonyl groups in the oxidation products of COS and Glc5. Using reductive amination, we successfully grafted Glc5 with the amino chromophores *p*-toluidine (*p*T) and rhodamine 123 (RHO123), showing that this approach effectively expands the COS chemical space, providing access to a wide range of interesting cello-conjugates for diverse applications.

2. Materials and methods

2.1. Substrates and enzymes

Methyl β-D-cellobiose (me-β-Glc2), and D-cellopentaose (Glc5) were purchased from Carbosynth (United Kingdom). D-cellobiose (Glc2) was from Roth Sochiel (France). 2,2-azino-bis(3-ethylbenzothiazoline-6-sulphonic acid) (ABTS), 2,2,6,6-Tetramethyl-1-piperidinyloxy (TEMPO), the laccase from *Trametes versicolor* (TvL) (E.C. 1.10.3.2), the cellulase cocktail (from *Trichoderma reesei*) ≥700 units/g, Avicel® PH-101, *p*-toluidine (*p*T), 2-picoline borane (pic-BH_3) and rhodamine 123 (RHO123) were purchased from Sigma-Aldrich (St Quentin Fallavier, France). Pellicon® XL50 with Ultracel® 30 kDa membrane was from Merck (Darmstadt, Germany).

2.2. Diafiltration of the laccase from Trametes versicolor

Discontinuous diafiltration was performed using a labscale TFF system (Merck KGaA, Darmstadt, Germany) with a Pellicon XL filter PXC030C50 (30 kDa) regenerated cellulose membrane (filter area 50 m^2) at a fixed transmembrane pressure of 2.1 bar at 4°C. The feeding chamber was filled with 50 mL of a solution of TvL at 30 g/L. The enzyme solution was diafiltrated twice with 500 mL of water or 20 mM acetate buffer pH 6.0, and then concentrated to 15 mL final volume. Before diafiltration, the membrane was previously rinsed with 20 mM acetate buffer pH 6.0 for 15 min. After each trial, the membrane was flushed with distilled water and stored in 50 mM NaOH. Diafiltrate and retentate were analyzed by HPAEC-PAD analysis.

2.3. Laccase activity

Laccase activity was determined using a colorimetric assay and 2,2-azino-bis(3-ethylbenzothiazoline-6-sulphonic acid) (ABTS) as a substrate. A volume of 10 µL of laccase solution at 0.1 mg/mL, 50 µL of 1 mM ABTS was mixed with 440 µL of acetate buffer (20 mM, pH 3.5). ABTS oxidation was monitored by measurement of the absorbance at 420 nm (ε_{420}= 3.6 × 10^4 M^{-1} cm^{-1}) and 30 °C using a UV-vis spectrophotometer Cary 100 Bio (Agilent Technologies, Santa Clara, CA, United States). One unit (U) of laccase activity is defined as the amount of laccase that oxidizes 1 µmol of ABTS per minute.

2.4. Preparation of a mix of COS

To produce COS, we used a protocol based on Avicel®PH-101 acid hydrolysis, which was adapted from Zhang & Lynd (2003). Briefly, Avicel® PH-101 (2.5 g) was suspended in cold HCl 37 % (20 mL) and in cold H_2SO_4 98 % (3.7 mol/L) (5 mL) in an Erlenmeyer flask. The reaction was carried out at room temperature during 2h30 and stirred with a magnetic stir bar. The hydrolyzate was precipitated with acetone at -20 °C (225 mL) and the solution was kept at -20 °C for 2h. The precipitate was recovered by centrifugation at 3500 rpm for 8 min at 4 °C and washed with acetone at -20°C (50 mL) and centrifuged. The pellet was dissolved in water (300 mL) and centrifuged at 5000 rpm for 8 min at 4°C to obtain a supernatant containing soluble COS. The COS solution was neutralized to pH 7 with $Ba(OH)_2$, and the precipitate of $BaSO_4$ formed was removed by centrifugation (10 000 rpm, 8 min at 4 °C). The residual acetone was evaporated and the soluble COS was freeze-dried to form a white powder. To remove the salts, the COS mixture (1 g) was dialyzed overnight against distilled water using 100-500 Da cut-off dialysis tubing from Biotech CE.

2.5. Oxidation of COS

Oxidation of D-cellobiose (Glc2), methyl β-D-cellobiose (me-β-Glc2) and COS was performed using 54 mM Glc2 or me-β-Glc2 or 17.2 g/L of a mix of cellooligosaccharides, 6 mM TEMPO and 5.4 U/mL of TvL (purified or not) in 20 mM acetate buffer at different pH values (3.0-6.0) and at 30°C (or 25°C). The reaction mixture (5mL) was stirred at 500 rpm (or not stirred) with a magnetic bar in open flask. Samples of 250 µL were collected during 24h for analyses. Either TvL (54 U), TEMPO (9.34 mg) or both were also added to attempt reaction restart after 8h of the reaction, which was initially carried out in 5mL volume with 54 mM Glc2 or me-β-Glc2 and at pH 6 and 30°C. Oxidation of Glc5 was carried out on 5 mL volume with 1.2 mM Glc5, 0.6 mM of TEMPO and 0.27 U/mL of the purified TvL in 20 mM sodium acetate buffer (pH 6.0) at 30 °C under 500 rpm stirring. Samples (250 µL) were taken periodically for 8h. For all oxidation reactions, TvL was inactivated by heating at 95 °C for 5 min. Three control experiments were conducted in parallel: control 1 with TvL and TEMPO, control 2 with COS and TEMPO, control 3 with COS and TvL.

2.6. Purification of oxidized products 2a and 2b

Products 2a and 2b were isolated by chromatography using an Agilent 1260 Infinity chromatographic system equipped with a Refractive Index detector (RI) and a Thermo Scientific™ Dionex UltiMate™ 3000 automate fraction collector (Thermo Fisher Scientific, San Jose, CA, USA). Analysis was

performed with a Shodex™ Asahipak NH2P-50 4E column (5 µm, 19 × 250 mm) maintained at 40 °C at a flow rate of 1 mL/min. Samples (50 µL) were injected and eluted with a solvent composed of water/ammonium acetate (0.3 M), 80:20 (v/v). The fractions containing 2a and 2b were collected and their purity was checked by HPAEC-PAD analysis before lyophilization.

2.7. NMR characterization of products 2a and 2b

For ^{1}H and ^{13}C NMR analyses, 1.5 mg of pure products 2a and 2b were dissolved in 150 µL D_2O containing sodium 2,2,3,3-tetradeuterio-3-trimethylsilylpropanoate (TSP-*d4*) and acetone as internal standards. The chemical shifts were calibrated with respect to TSP-*d4* ($\delta^{1}H$ 0.00 ppm) and acetone ($\delta^{13}C$ 30.89 ppm). ^{1}H and ^{13}C NMR spectra were recorded on a Bruker Avance 500-MHz spectrometer operating at 500.13 MHz for ^{1}H NMR and 125.75 MHz for ^{13}C using a 5-mm z-gradient TBI probe. 1D and 2D NMR (COSY, HSQC, HMBC) were recorded in the same conditions in 3 mm tube at 298 K. Data were processed using TopSpin 3.6.2 software.

2.8. Grafting of aminated compounds onto oxidized cellopentaose

Glc5 (27 mM) was oxidized using 0.6 mM of TEMPO and 5.4 U/mL of TvL in acetate buffer (20 mM, pH 6.0) at 30°C for 8h. The reaction medium (500 µL) was then incubated with 10.15 mM of *p*-toluidine (*p*T) or rhodamine 123 (RHO123), 2.43 mM of 2-picoline borane (pic-BH_3) and 10 % of acetic acid for 3 h at 40 °C under stirring at 500 rpm. Then, the reaction mixture was centrifugated for 5 min at 10 000 rpm before being diluted for LC-HRMS analysis. After grafting with *p*T or RHO123, the pH of the reaction mixture (500 µL) was adjusted to 4.8 with 2M NaOH before addition of 80 µL of a cellulase cocktail from *T. reesei* (≥700 units/g). Enzymatic hydrolysis was carried out for 24 h at 40 °C and 500 rpm agitation, the reaction was stopped by heating the samples for 10 min at 95 °C. The samples were centrifugated 5 min at 5 000 rpm and filtered on 0.45 µm membrane before HPLC analysis.

2.9. Analyses of oxidized oligosaccharides

HPAEC-PAD analysis. High performance anion exchange chromatography with pulsed amperometric detection (HPAEC-PAD) analysis was carried out using a Dionex™ ICS-6000 DC (Thermo Fischer Scientific, San Jose, CA, USA) equipped with a Dionex™ CarboPac™ PA100 analytical column (2 x 250 mm) at a flow rate of 0.25 mL/min. The mobile phase was A: NaOH 150 mM and B: NaOH 150 mM with 500 mM sodium acetate. The injection volume of the reaction mixture obtained after LMS

oxidation was set at 10 µL. Solvent A was applied for 5 min and the products were eluted using a gradient from 0 to 40% of B over 35 minutes. Before analysis, reaction mixtures obtained from Glc2 (54 mM) were diluted 667 times in water and those obtained from me-β-Glc2 (27 mM) or Glc5 (1.2 mM) oxidation 40 times. A linear calibration curve was generated for Glc2, me-β-Glc2 and Glc5 using concentrations of commercially available standards in the range of 5 to 30 mg/L. Data acquisition and processing were performed using Chromeleon™ 7.2 data software.

HPLC-CAD analysis. High performance liquid chromatography with charged aerosol detection (CAD) analysis of the reaction mixture obtained with Glc2, me-β-Glc2 or Glc5 were performed using a Thermo Scientific™ UltiMate™ 3000 system, (Thermo Fisher Scientific, San Jose, CA, USA) with a Shodex™ Asahipak NH2P-50 4E (5 µm, 4.6 mm x 250 mm) column at 40 °C and at a flow rate of 1 mL/min. Samples were not diluted. The mobile phase was composed of solvent A: acetonitrile, B: water and C: ammonium acetate (0.3 M). A gradient starting with solvent A-B 75/25 and decreasing to A-B 40/60 over 30 min was first applied to elute the neutral sugars. Then, solvent B 100% was applied in isocratic mode for 10 min. The oxidized compounds were finally eluted with a step-gradient comprising four steps of 10 min each: step 1 B-C 90/10; step 2 B-C 80/20; step 3 B-C 70/30 and step 4 B-C = 0/100. Finally, the column was re-equilibrated during 10 min with A/B =75:25.

HPLC-MS analysis of Glc2 and me-β-Glc2 was performed using an Ultimate 3000 series chromatograph equipped with a Dionex 340 UV/VIS detector coupled with a simple quadruple mass spectrometer (MSQ Plus, Thermo Fisher Scientific) with a Shodex™ Asahipak NH2P-50 4E column (5 µm, 4.6 × 250 mm) maintained at 40°C. Samples (50 µL) were analyzed by isocratic elution with water-ammonium acetate (0.3 M), 80:20 at a flow rate of 1 mL/min for 20 min. Mass detection was carried out in a positive and negative heated electrospray ionization (ESI) mode. Mass spectrometer settings were as follows: the spray voltage was 3.5 kV, the voltage cone at 60 V, the temperature of ESI ion source was 350 °C and the gas carrier was nitrogen. The mass spectrometer scanned was from m/z 100 to 1 900. Data acquisition and processing were performed using Chromeleon™ 7.2 data software.

HPLC-HRMS of Glc2 and me-β-Glc2 analyses were carried out on a Vanquish™ system coupled to a Thermo Scientific Q Exactive™ Plus hydrid quadrupole-Orbitrap™ mass spectrometer (Thermo Fisher Scientific) with a column Shodex™ Asahipak NH2P-50 4E (5 µm, 4.6mm x 250 mm) equipped with a Shodex™ Asahipak NH2P-50 4A guard column (4.6 x 10 mm) at a flow rate of 0.5 mL/min. The column and autosampler temperature were set at 40 °C and 4 °C, respectively. Samples were analyzed using the following gradient of A-B 20 mM ammonium acetate-acetonitrile (25/75 at 0 min, 60/40 at 10 min, 60/40 at 15 min and 100 % A at 25 min). Injection volume was set at 10 µL. Conditions for ESI in

negative mode were as follows: spray voltage was at 2.75 kV, and capillary and desolvation temperatures were of 400 °C. The maximum injection time was 100 ms. Nitrogen was used as the sheath gas (pressure, 75 units) and auxiliary gas (pressure, 20 units). The automatic gain control (AGC) was set at 10^6 for full-scan mode, with a mass resolution of 70 000 (at 400 m/z). For the full scan MS analysis, the spectra were recorded in the range of m/z 80-1 000. Finally, data acquisition was performed using Thermo Scientific Xcalibur software 4.1.

IC-HRMS analysis of oxidized Glc5. The mass of Glc5 oxidation products were determined using a liquid anion exchange chromatography on Dionex™ ICS-5000+ Reagent-Free™ HPIC™ system (Thermo Fisher Scientific™, Sunnyvale, CA, USA), coupled to a Thermo Scientific™ LTQ Orbitrap Velos™ mass spectrometer (Thermo Fisher Scientific, San Jose, CA, USA) equipped with a heated electrospray ionization probe and equipped with an eluent generator system (ICS-5000+EG, Dionex) for automatic base generation (KOH). Analytes were separated within 50 min, using a linear KOH gradient elution applied to an IonPac AS11-HC column (250 x 2 mm, Dionex) equipped with an AG11-HC guard column (50 x 2 mm, Dionex) at a flow rate of 0.38 ml/min. The gradient program was following: equilibration with 7 mM KOH during 1 min; then KOH ramp from 7 to 15 mM, from 1 to 9.5 min; constant concentration 10.5 min; ramp to 45 mM in 10 min; ramp to 70 mM in 3 min; ramp to 100 mM in 0.1 min; constant concentration 8.9 min; drop to 7 mM in 0.5 min; and equilibration at 7 mM KOH for 7.5 min. The column and autosampler temperatures were thermostated at 25 °C and 4 °C, respectively. The injected sample volume was 15 µl. Conditions for electrospray ionization (ESI) in negative mode were as follows: spray voltage was at 2.7 kV, capillary and desolvation temperatures were fixed at 350 °C and the maximum injection time was 50 ms. Nitrogen was used as the sheath gas (pressure, 50 units) and auxiliary gas (pressure, 5 units). AGC was set at 10^6 for full-scan mode, with a mass resolution of 60 000 (at 400 m/z). For the full scan MS analysis, the spectra were recorded in the range of m/z 80.0-1 000.0. Finally, data acquisition was performed using Thermo Scientific Xcalibur software 2.2 SP1.

LC-HRMS/UV analysis of cellopentaose grafted with *p*-toluidine or rhodamine 123. Analyses were carried out on a Vanquish™ system coupled to a Thermo Scientific Q Exactive™ Plus hydrid quadrupole-Orbitrap™ mass spectrometer (Thermo Fisher Scientific). Samples were separated within 95 min using an isocratic elution with a mixture containing 10 % acetonitrile-40 % water-50 % 20 mM ammonium acetate applied to a Shodex™ Asahipak NH2P-50 4E (5 µm, 4.6 mm x 250 mm) column equipped with a Shodex™ Asahipak NH2P-50 4A guard column (4.6 x 10 mm) at a flow rate of 0.7 mL/min. The column and autosampler temperatures were set at 40 °C and 4 °C, respectively. Injection volume was of 10 µL. UV/Vis detection was performed at 286 nm for the samples grafted with *p*-toluidine and 500 nm for those grafted with rhodamine 123. ESI in negative mode was

performed with spray voltage at 2.75 kV, and capillary and desolvation temperatures of 400 °C. Maximum injection time was 100 ms. Nitrogen was used as the sheath gas (pressure, 75 units) and auxiliary gas (pressure, 20 units). AGC was set at 10^6 for full-scan mode, with a mass resolution of 70 000 (at 400 m/z). For the full scan MS analysis, the spectra were recorded in the range of m/z 80-1 000. Finally, data acquisition was performed using Thermo Scientific Xcalibur software V.

LC-MS/MS analysis.MS/MS analyses of Glc5 grafted with *p*-toluidine were performed on MetaToul-Axiom platform facility at INRAE Toulouse with a Thermo Scientific™ LTQ Orbitrap XL™ mass spectrometer (Thermo Fisher Scientific, San Jose, CA, USA) coupled with an UV detector. Reaction media were diluted 250 times in water-acetonitrile (95.5:4.5, v/v). Separation was performed with a Shodex™ Asahipak NH2P-50 4E (5 µm, 4.6 x 250 mm) column equipped with a Shodex™ Asahipak NH2P-50 4A guard column (4.6 x 10 mm) placed in an oven at 40 °C. Injection was set at 10 µL. Elution was performed isocratically with a water-ammonium acetate 20 mM-acetonitrile mixture (40:50:10, v/v/v) at a flow rate of 700 µL/min. Mass detection was carried out in negative mode over mass ranges of m/z 80 – 1200 in MS mode and m/z 245-950 in MS/MS mode. Spray voltage was set at 2.75 kV. MS/MS analyses in collision-induced dissociation were performed by selected the mass of the precursors of interest as $[M-H]^-$ at m/z 932.32 in the quadrupole prior to their fragmentation in the transfer cell of the instrument (collision energy adjusted at 30 V). Argon was used as the collision gas. UV-detection was set at 286 nm. Data acquisition was carried out using the Xcalibur software. Annotations of spectra and structures were performed according to the nomenclature of Domon and Costello (1988).

MALDI-TOF-MS analysis of mix of COS*.* Mass spectra were recorded on a Waters Micromass MALDI micro MX mass spectrometer. The measurements were performed with the mass spectrometer in positive reflection mode using an accelerating voltage of 12 kV. Mass spectra were acquired from 550 (m/z) to 3000 (m/z). COS were dissolved in water (1 mg/mL) and mixed with the DHB matrix solution (2.5-dihydroxybenzoic acid, 10 mg/mL in H_2O:EtOH, 0.5:0.5; v/v) and NaI solution (sodium iodide 10 mg/mL in H_2O:EtOH, 0.5:0.5, v/v). Samples were prepared by mixing COS solutions, matrix solution, and the cationization agent solution in the ratio 1:3:1 (v/v/v). A total of 1 µL was applied to a stainless steel sample slide and dried at room temperature.

3. Results and discussion

To develop an eco-friendly process to graft aminated substances onto COS, we applied the protocol described in (Scheme 1), starting with the oxidation of COS using LMS followed by a direct reaction with an amino-chromophore to form a Schiff base with an imine bond. The imine bond was subsequently reduced using 2-picoline borane to generate a more stable C-N bond. The *Trametes versicolor* laccase and TEMPO couple, already used for cellulosic pulp oxidation (Patel et al., 2011), was first tested to oxidize D-cellobiose (Glc2), methyl β-D-cellobiose (me-β-Glc2), a mixture of COS and D-cellopentaose (Glc5). With LMS, the laccase-oxidized redox mediator, in our case $TEMPO^+$, is responsible for sugar oxidation.

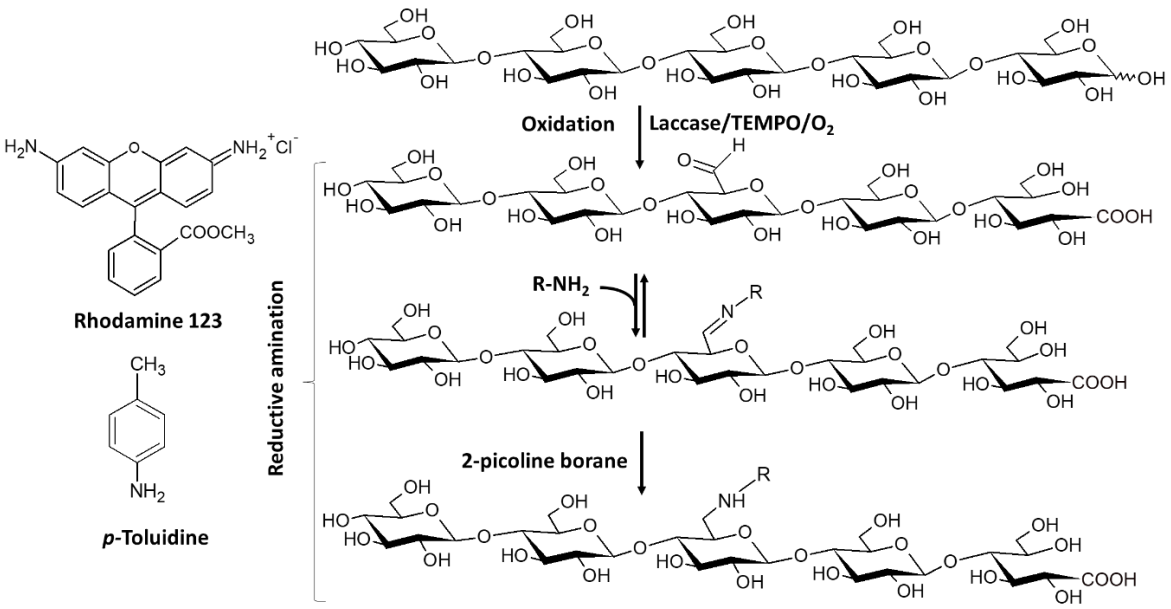

Scheme 1. Two-step chemo-enzymatic procedure for the preparation of cellooligosaccharide-conjugates using the laccase/TEMPO/O_2 system for carbohydrate oxidation followed by the reductive amination with amino-chromophores.

3.1. Oxidation of cellobiose and methyl cellobiose using the laccase/TEMPO/O_2 system

We first performed the oxidation of Glc2 and me-β-Glc2. The product profiles obtained after 8 and 24 h oxidation enabled the identification of product 1a (at t_r=57.9 min with m/z 376 $[M+NH_4]^+$) corresponding to the aldonic acid form (C_1OOH) of Glc2 (Fig. 1A). With me-β-Glc2, two oxidation products 2a and 2b were obtained (at t_r=56.3 and 57.0 min) both with m/z 388 $[M+NH_4]^+$ (Fig. 1B).

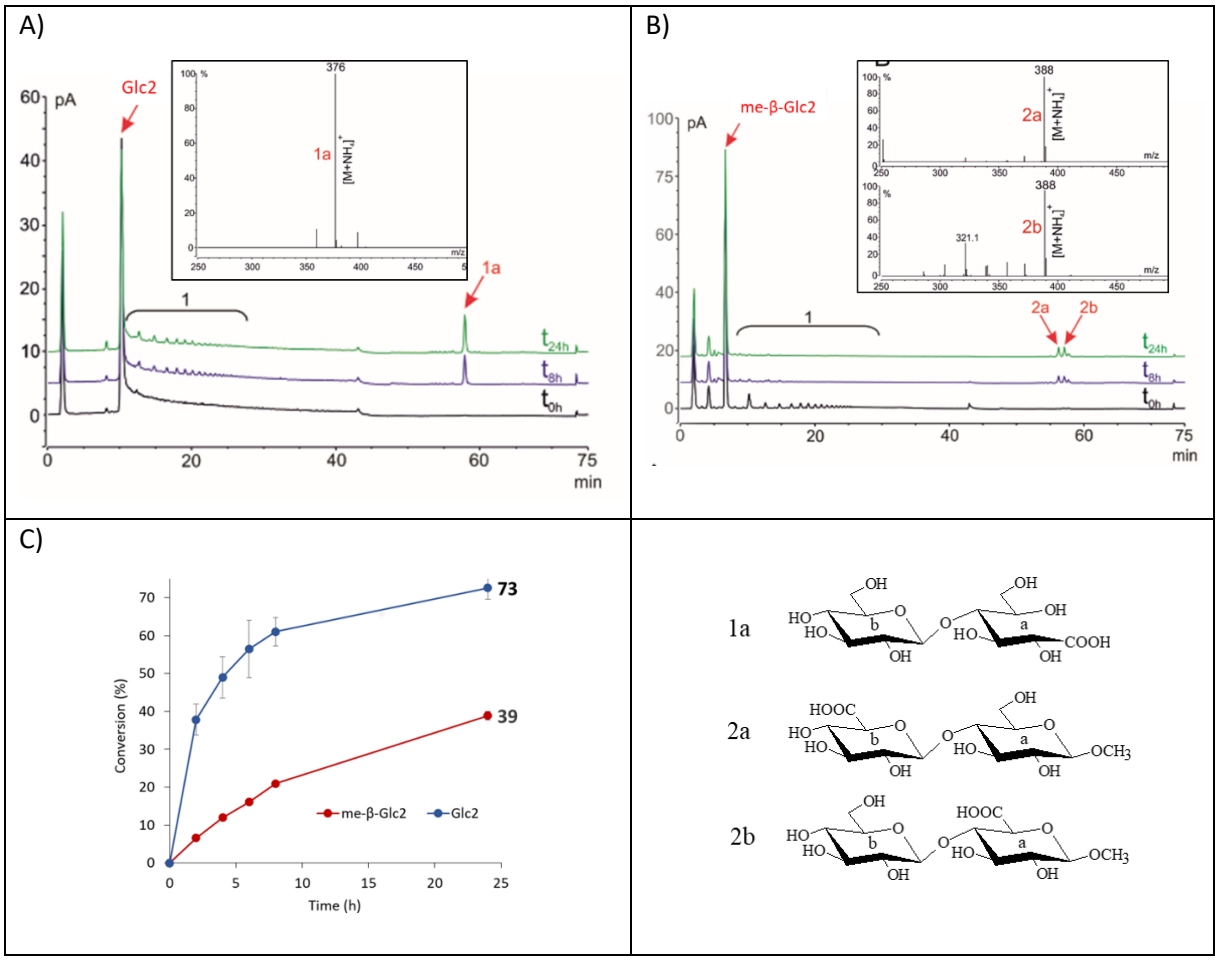

Fig. 1. Oxidation of Glc2 or me-β-Glc2 with LMS system. (A) HPLC-CAD chromatograms of reaction mixture with Glc2; 1= maltooligosaccharides (t_r between 5-26 min present in commercial preparation of TvL); 1a monoacid formed during the reaction t_r=57.9 min and ESI-mass spectrum, m/z 376 $[M+NH_4]^+$. (B) HPLC-CAD chromatograms of reaction mixture with me-β-Glc2; 1= maltooligosaccharides (t_r= 5-26 min); 2a and 2b monoacid formed during the reaction, 2a t_r= 56.3 min**,** 2b t_r= 57.1 min and ESI-mass spectra of 2a and 2b**,** m/z 388 $[M+NH_4]^+$. (C) Glc2 and me-β-Glc2 conversion versus reaction time, conversions were determined by HPAEC-PAD analysis. Reaction conditions: 54 mM Glc2 or me-β-Glc2 TEMPO 6 mM, TvL 5.4 U/mL, 10 mL sodium acetate buffer (20 mM; pH 4.5), 30°C, 24 h, 500 rpm. The experiments have been carried out in triplicates and some standard deviation are too small to be visualized. In the control experiments without laccase or without TEMPO, no oxidation products were detected (data not shown).

The mass increase (m/z +14) indicates the presence of one carboxyl group on C-6 of the a or b glucosyl ring of me-β-Glc2. The structures of 2a and 2b, isolated with a purity higher than 98% were determined using 1D-, 2D-NMR analyses (Fig. S1, S2, Table S1). In the ^{13}C-NMR spectrum of 2a and 2b, the signals of the primary C-6 OH of me-β-Glc2 at 61.2 ppm and 60.6 ppm disappeared to the profit of the characteristic signals of C-6 carboxylic acid group at 176.1 ppm and 175.7 ppm for 2a and 2b, respectively (Fig. S2B). 2D-NMR confirms that 2a and 2b are oxidized on the C6 of glucosyl ring b and a of me-β-Glc2, respectively. Conversion of Glc2 was fivefold faster than that of me-β-Glc2 and a maximum conversion of 73% and 39% was reached after 24 h reaction for Glc2 and me-β-Glc2,

respectively (Fig. 1C). This can be explained by the higher reactivity of the C1 aldehyde of Glc2 compared to the C6-hydroxyl of me-β-Glc2. HPLC-CAD analysis also revealed traces of oligosaccharides in the control reaction (with only TvL and TEMPO, Fig. 1A, 1B), corresponding to maltooligosaccharides (MOS) contained in the laccase preparation (Fig. S3 A). To avoid any interferences between COS and MOS oxidation, we prepared a MOS-free preparation of the commercial laccase by diafiltration and used it in the following experiments (Fig. S3B).

To date, oligosaccharide or polysaccharide oxidation with Laccase/TEMPO system has mainly been performed under acidic conditions at pH 4.5 to 5.0 (Jaušovec et al., 2015; Marzorati et al., 2005; Quintana et al., 2017). As chemical oxidation with TEMPO is more efficient under basic conditions, we increased the reaction pH to 6 after verifying that TEMPO (alone) was sufficiently oxidized to oxoammonium ($TEMPO^+$) at pH 6 (figure S4). Remarkably, me-β-Glc2 conversion was four times faster at pH 6 than at any other pHs increasing from 40 % to 62 % (Fig. 2A). Regardless of reaction pH, a plateau is reached - after 8 h at pH 6 and 24 h at pH 3.5 and 4.5 - which may be due to either enzyme inactivation or TEMPO ($TEMPO^+$) oxidation as described by Jiang et al. (2021). Stirring at 500 rpm enabled us to further increase me-β-Glc2 conversion value from 58% (without stirring) to 69%, probably owing to better oxygen supply (Fig. 2B). The me-β-Glc2/TEMPO molar ratio is also an important parameter to consider. Oxidation is faster at me-β-Glc2/TEMPO molar ratio 9 (54 mM/6 mM) in comparison to a ratio of 4.5 (27 mM/6 mM) but the best conversion (77 %) is obtained with a ratio of 4.5. (Fig. 2C). Over 8h, conversion varied very little. As shown in Fig. 2D, the addition of laccase (54 U), TEMPO (9.34 mg) or both resulted in an inflexion in the reaction rate decrease, and conversion resumed upon complete consumption of me-β-Glc2, 16 h after addition, with a concomitant decrease in pH (Fig. S5). This indicates that the enzyme initially used may have been partially inactivated, limiting $TEMPO^+$ formation and carbohydrate oxidation. The addition of $TEMPO^\bullet$ also restarted the reaction, showing that at least some of the initially introduced enzyme was still active in oxidizing $TEMPO^\bullet$ to $TEMPO^+$. Altogether, these results suggest that $TEMPO^+$ was the limiting reagent, due to ion instability or to the slow regeneration of $TEMPO^\bullet$ from TEMPOH under acidic pH as reported by Arends et al. (2006).

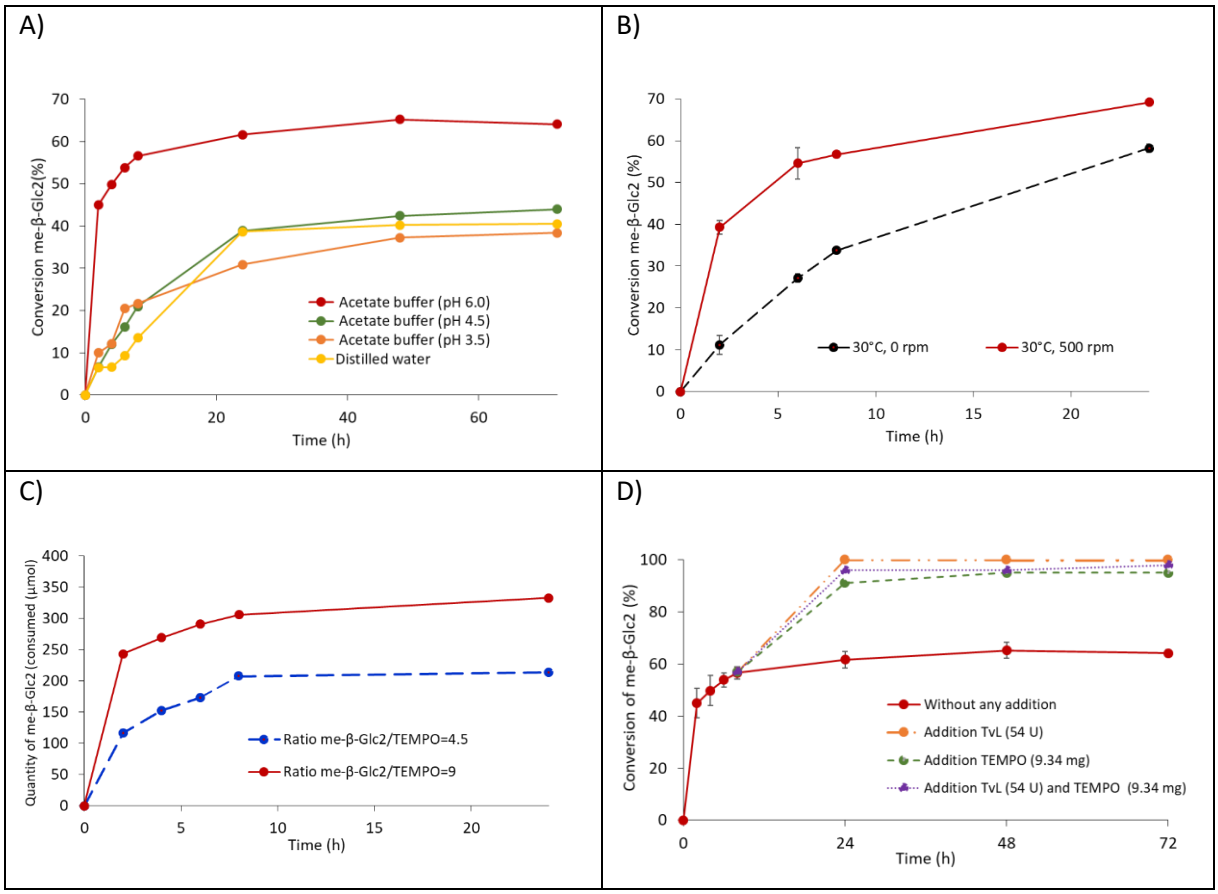

Fig. 2. Effect of pH (A), agitation (B) and sugar/TEMPO molar ratio (C) on conversion of me-β-Glc2. The me-β-Glc2 conversion was determined by HPAEC-PAD analysis. Reaction conditions: (A) oxidation of me-β-Glc2 was performed in 20 mM sodium acetate buffer at pH 3.5, 4.5 and 6.0 or in distilled water (pH 6.5) with 54 mM me-β-Glc2 (540 µmol), 6 mM TEMPO (60 µmol), 5.4 U.mL^{-1} TvL under 500 rpm or (B) without agitation, sodium acetate buffer at pH 6.0) at 30°C in open flask ;(C, D) me-β-Glc2 54 mM or 27 mM (540 or 270 µmol), TEMPO 6 mM, TvL 5.4 U/mL (54 U), volume 10 mL (sodium acetate buffer 20 mM, pH 6), 500 rpm,30 °C in open flask. (D) conversion progress after addition of TvL, TEMPO, or both after 8 h reaction. The experiments have been carried out in triplicates and some standard deviation are too small to be visualized.

3.2. Oxidation of COS

3.2.1. Oxidation of a mixture of COS

We first produced a mixture of COS with degrees of polymerization ranging from 1 to 13 by acid hydrolysis of Avicel®PH-101 (Fig. S6) and then applied to COS the protocol used for me-β-Glc2 oxidation. HPLC profiles (Fig. S7A, S7B) and MALDI-TOF analyses of the reaction products revealed the presence of oxidized compounds (Fig. 3A). MALDI-TOF spectrum of the DP6 at m/z 1 013 ([M+Na]$^+$) (Fig. 3B, Table 1) reveals several different ions with m/z-values varying slightly compared to the unoxidized DP6 (Fig. S6B). These ions could be attributed to different structures and only mass spectrometry fragmentation could help to discriminate more precisely the structures obtained. However, the peak at m/z 1 011 indicates that carbonyl functions are formed, which augurs well for

subsequent functionalization with compounds bearing an amine group. In addition, given the specificity of $TEMPO^+$ for oxidation of aldehyde and primary hydroxyl groups, we can assume that oxidation occurred mainly on the C-1 at the reducing end or on the C-6 of the different rings of DP6, which is interesting for functionalization with an amine group-bearing substituent.

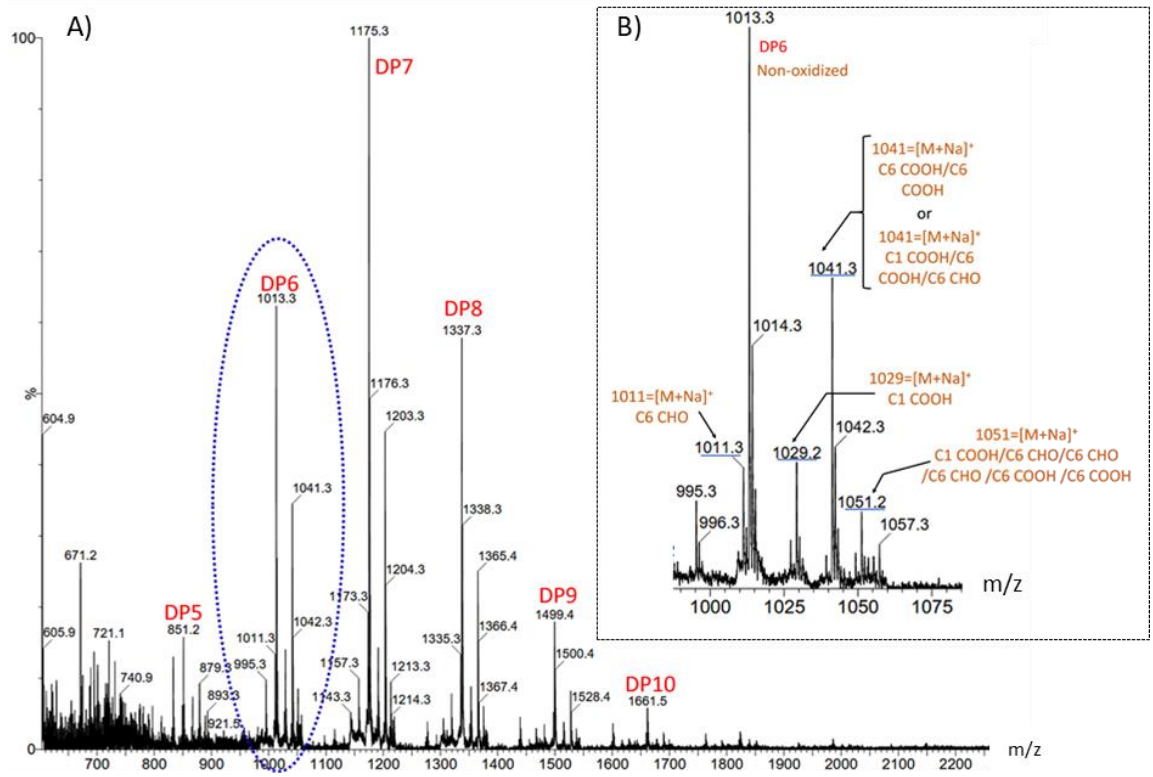

Fig. 3. MALDI-TOF spectrum (DHB matrix with NaI salt in positive mode) of oxidized COS (DP 1-13). (A) After oxidation with laccase/TEMPO System. (B) Zoom on the DP6. In brown, are given some examples of the structural modifications due to oxidation. The reaction was carried out with 17 mg/mL of substrate, 54 U of laccase from Tvl and 0.6 mM of TEMPO in 5 mL acetate buffer (20 mM, pH 4.5) at 30 °C for 24 h.

Table 1. Mass of the oxidized products formed from DP6 COS oxidation determined by MALDI-TOF analysis.

m/z detected $[M+Na]^+$	Assignment of possibly introduced oxidized functions*
m/z = 1013	DP6 (non-oxidized)
m/z = 1011	m/z DP6 - 2: presence of one carbonyl group on the C-6, C-3 or C-2 of one of the ring *a*, *b*, *c*, *d*, *e* or *f* of DP6
m/z = 1029	m/z DP6 + 16: presence of C_1OOH, in ring *a* or geminal diols at C-2, C-3, or C-6 of rings *a*, *b*, *c*, *d*, *e* or *f*
m/z = 1041	m/z DP6 + 14 + 14: presence of two carboxylic acid groups in the DP6 or presence of one C_6HO, one C_6OOH and C_1OOH (m/z DP6 - 2 + 14 + 16). Many other combinations could match with a mass increase of 28
m/z = 1051	m/z DP6 (- 2) x3 + (14) x2 + 16: possible presence of three carbonyl groups, two carboxyl groups (C_6OOH) and carboxyl group on C-1 in the DP6. Many other profiles of oxidation could match with this mass increase

* The m/z values were compared to m/z 1013 ($[M+Na]^+$) of DP6 (M=990 Da)

3.2.2 Oxidation of cellopentaose

In order to facilitate structural analysis of the oxidation products and their derivatives resulting from subsequent functionalization, we chose to oxidize pure Glc5 and monitored the reaction by HPAEC-PAD analysis (Fig. 4A-D). We obtained 41 % conversion and reached a plateau after 4 h of reaction, indicating laccase inactivation and/or a problem of $TEMPO^{\bullet}$ regeneration at acidic pH as previously seen for me-β-Glc2 oxidation (Fig. 4A). HPAEC-PAD chromatogram revealed the presence of 5 products that can be attributed to product 3c (t_r= 22.92 min) and of at least four minor products of oxidation (Fig. 4B). Their structure was further investigated by ion exchange chromatography-high resolution (Orbitrap) mass spectrometry (IC-HRMS). Based on the extracted ion chromatogram (Fig. 4C), the product 3c m/z 843.26 ($[M-H]^-$) with a m/z +16 mass increase relative to that of Glc5 m/z 827.27 ($[M-H]^-$) could be a C-1-oxidized Glc5 (aldonic acid form) or a Glc5 with a geminal diol (hydrated aldehyde or ketone) at C-2, C-3 or C-6 position of its glucosyl ring. The products 3d m/z 841.24 ($[M-H]^-$) and 3b m/z 863.24 ($[(M-H+Na)-H]^-$), both with a m/z +14 mass increase are consistent with the presence of a carboxyl group at the C-6 position in one of the Glc5 glucosyl rings, with five positional isomers possible. It can also reflect, for example, the occurrence of an aldonic acid at C-1 plus a carbonyl group at C-2, C-3 or C-6 position in one of the Glc5 rings. The presence of a geminal diol (m/z +16 mass increase) and a carbonyl (m/z -2 mass decrease) in the Glc5 could also explain the m/z +14 mass increase and cannot be excluded. No species with only one carbonyl group (m/z -2

mass decrease) were detected. In summary, several structures of oxidized products account for the variations of mass observed. It is not possible to distinguish these isomers without additional analyses. However, in products 3b or 3d, we clearly demonstrate that a carbonyl group is present in addition to a carboxyl or geminal diol group, a new result never before reported for oligosaccharide oxidation opening up good prospects for future reductive amination. Oxidation of insoluble cellulose nanofibers, cellulosic fibers or fabrics by LMS with TEMPO also resulted in the formation of carboxyl and carbonyl groups due to C6-OH oxidation. The ratio of -COOH to -CHO was shown to be influenced by the type and amount of laccase, mediator and substrate, as well as by the reaction conditions (Jaušovec et al., 2015; Jiang et al., 2017, 2021; Patel et al., 2011; Quintana et al., 2017). In soluble COS, COOH groups were mainly introduced. It is likely that by adjusting the reaction conditions, the carbonyl content can be increased, as is the case with insoluble material.

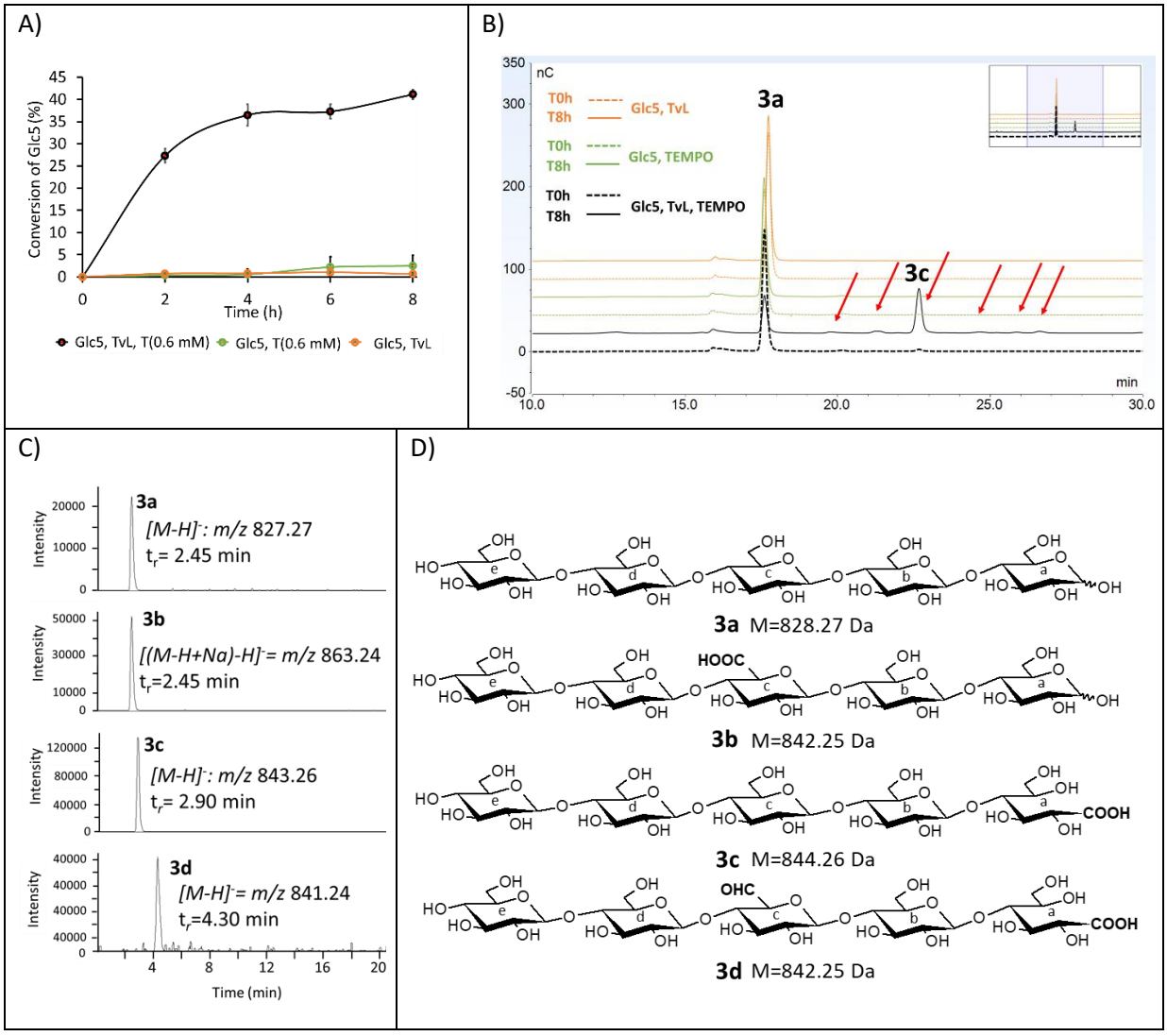

Fig. 4. Oxidation of cellopentaose (Glc5) by laccase/TEMPO system. (A) Glc5 conversion versus reaction time, conversions were determined by HPAEC-PAD analysis. (B) HPAEC-PAD profiles of Glc5 oxidation products. Control without TEMPO and control without laccase are shown in orange and green, respectively. The main product 3c (t_r = 22.92 min) and other minor products are showed by red arrows. (C) Extracted ion chromatograms of oxidized products after ionic chromatography high mass spectrometry in negative mode. (D) Glc5 and potential structures of oxidized Glc5 products and their calculated molecular mass. The carbonyl (3d^c) and carboxylic acid (3b^c) groups are arbitrarily placed on glucose unit '*c*'. Reactions performed with Glc5 (1.2 mM, 6 µmol), TEMPO (0.3 mM, 1.5 µmol), laccase (0.27 U/mL) in 5 mL of acetate buffer (20 mM pH 6.0), open flask at 500 rpm, 30 °C, 8 h.

3.3. Grafting of amino compounds onto oxidized Glc5

The plan was to exploit the presence of a carbonyl group in the oxidized products to attempt reactions with the amine group of amino-chromophores, first synthesizing an imine (-C=N-) and then reducing it to give a secondary amine with a strong covalent bond between the substituent and the oligosaccharide (Scheme 1).

3.3.1 Grafting of p-toluidine

Reductive amination was first tested with *p*-toluidine (*p*T), directly on the oxidized Glc5. The amine (10 % (v/v)) was added along with 2-picoline borane (pic-BH_3) as a reductant, and contact was maintained for 3 h at 40 °C under stirring. Pic-BH_3 was chosen over the more usual $NaBH_3CN$, as it is a less hazardous reductant that prevents the production of toxic by-products such as cyanide residues (Sato, Sakamoto, Miyazawa, & Kikugawa, 2004). LC-HRMS analysis of the products in negative mode revealed several signals that can be attributed to functionalized derivatives (Fig. 5). Products, 4a' (t_r=3.45 min, m/z 916.33, $[M-H]^-$) and 4b (t_r=3.47 min, m/z 918.34, $[M-H]^-$) correspond to grafted Glc5 without carboxyl group. Product 4a' (m/z 916.33) with a m/z + 89 mass increase relative to Glc5 mass corresponds to a toluidine grafted to the C-2, C-3, or C-6 of one of the 5 glucose rings of Glc5, the grafting on the C-6 position being the most probable. Another possible structure for 4a would be a *p*T grafted to the C-1 plus an aldehyde group on the C-2, C-3 or C-6 of units a, b, c, d or e. Product 4b (m/z 918.34) with a m/z + 91 mass increase is a Glc5 with *p*T grafted at C-1 of unit a (reducing end), which supports the hypothesis that enzymatic oxidation of the reducing end was not complete, leaving the anomeric aldehyde free for subsequent reductive amination. The other products eluting after 30 min (4c, 4c', 4c'' and 4c''') have the same m/z value of 932.32 ($[M-H]^-$), with m/z +105 mass increase compared to Glc5. The m/z +105 increase can be broken down in m/z +89 and m/z +16 increase, accounting for a C-6-grafted toluidine (or C-2, C-3) on one of the Glc5 units, and a carboxyl group at the C-1 of Glc5 reducing end.

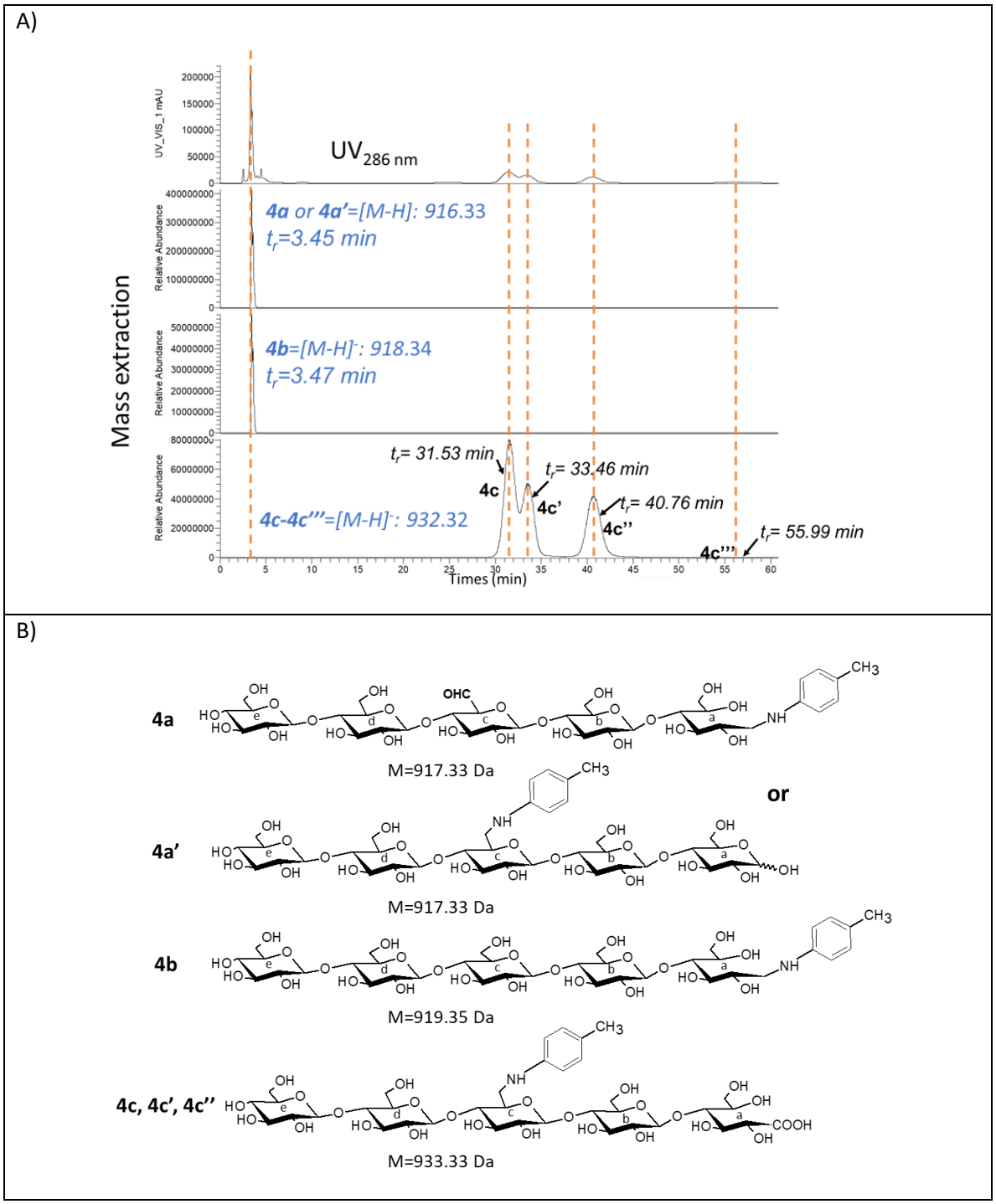

503 Fig. 5. LC-UV-HRMS analysis of the glucoconjugate obtained by reductive amination of oxidized Glc5
504 with toluidine. (A) UV_{286nm} chromatogram and extracted ion chromatograms of products 4a, 4a', 4b,
505 4c, 4c' and 4c''. (B) Potential structures of compounds 4 and their calculated molecular mass. In the
506 structures 4a, note that the carbonyl function could also be on the C-2, or C-3 of the glucosyl units,
507 similarly we cannot rule out the *p*T being grafted onto the C-2 or C-3, although these grafting
508 positions are less likely. Reaction conditions: after 8 h of enzymatic oxidation of Glc5 with
509 TvL/TEMPO, 500 µL of the oxidized reaction medium was mixed for 3 h with 10.15 mM pT, 2.43 mM
510 pic-BH_3 and 10 % acetic acid at 40 °C.

511

Given the complexity of the products obtained and the multiple structures that could match with the mass analysis, we turned to LC-HRMS/MS using collision induced dissociation fragmentation (CID-MS/MS) of the molecular ions at m/z 932.32, $[M-H]^-$ in negative mode to analyze the three most abundant isomers 4c (t_r= 31.53 min), 4c' (t_r= 33.46 min) and 4c'' (t_r= 40.76 min).

Annotation was performed according to the nomenclature developed by Domon & Costello (1988) (Fig. 6 A-C, Fig. S8). MS/MS fragmentation of the three molecular ions displayed mostly the same fragmentation patterns as those described by Sun et al. (2020) for C-1-oxidized cellooligosaccharides (Fig. 6 A-C, Fig. S8). Overall, B-/Y- and C-/Z-fragments arising from glycosidic bond cleavage are less abundant than those resulting from ring cleavage, such as $^{0,2}A_n$ and $^{2,4}A_n$ fragments, with the $^{2,4}A_n$ fragments overall dominating. The MS/MS spectra of the three isomers 4c, 4c' and 4c'' showed, among the most abundant fragments, a characteristic intracyclic fragment $^{2,4}A_5$ at m/z 796, confirming the grafting of *p*T on the C-6 or C-2 carbon atom of the glucose units *b*, *c*, *d*, or *e* or on the C-3 of glucose units *a*, *b*, *c*, *d*, or *e* or on C-4 of the glucose unit *e* with an aldonic acid residue on glucosyl unit *a*.

In addition to the fragment $^{2,4}A_5$, product 4c fragmentation yielded fragments B_3 (m/z 574), Y_4 (m/z 770) and the abundant fragment $^{2,4}A_4$ at m/z 634 (Fig. 6A). These fragments are matching with *p*T on units *c* or *d*. Due to i) the presence of a low signal intensity of the fragment at m/z 323, which could correspond to B_2 fragment without *p*T, ii) the B_2 fragment at m/z 412 and iii) the very low intensity of Y_3 (m/z 519), we cannot determine whether *p*T is linked to unit *c* or *d*, the two isomers could be present and coelute together.

In the case of product 4c' (Fig. 6B), the abundant fragment $^{2,4}A_4$ at m/z 545 and the fragment $^{2,4}A_5$ at m/z 796 with a mass increase of 162 and m/z + 89 (89 = mass of toluidine) plus the fragment B_4 at m/z 736 are consistent with pT bound at the C-6 of the glucosyl unit b. Although less probable, we cannot exclude pT binding at C-2 of unit b.

Regarding product 4c'' (Fig. 6C), a fragment Y_4 at m/z 681 is seen with a mass decrease of m/z 89 compared to the mass of fragment Y4 at m/z 770 observed from the fragmentation of products 4c and 4c'. This fragment plus the C_1 fragment at m/z 268 clearly indicates that *p*T is carried at the position C-6, C-2, C-3 or C-4 of glucosyl unit *e*. Other fragments such as $^{2,4}A_4$ (m/z 634), B_3 (m/z 574), $^{2,4}A_3$ (m/z 472) or the m/z 383 result from successive fragmentation $Y_4/^{2,4}A_4$ are consistent with the proposed structure.

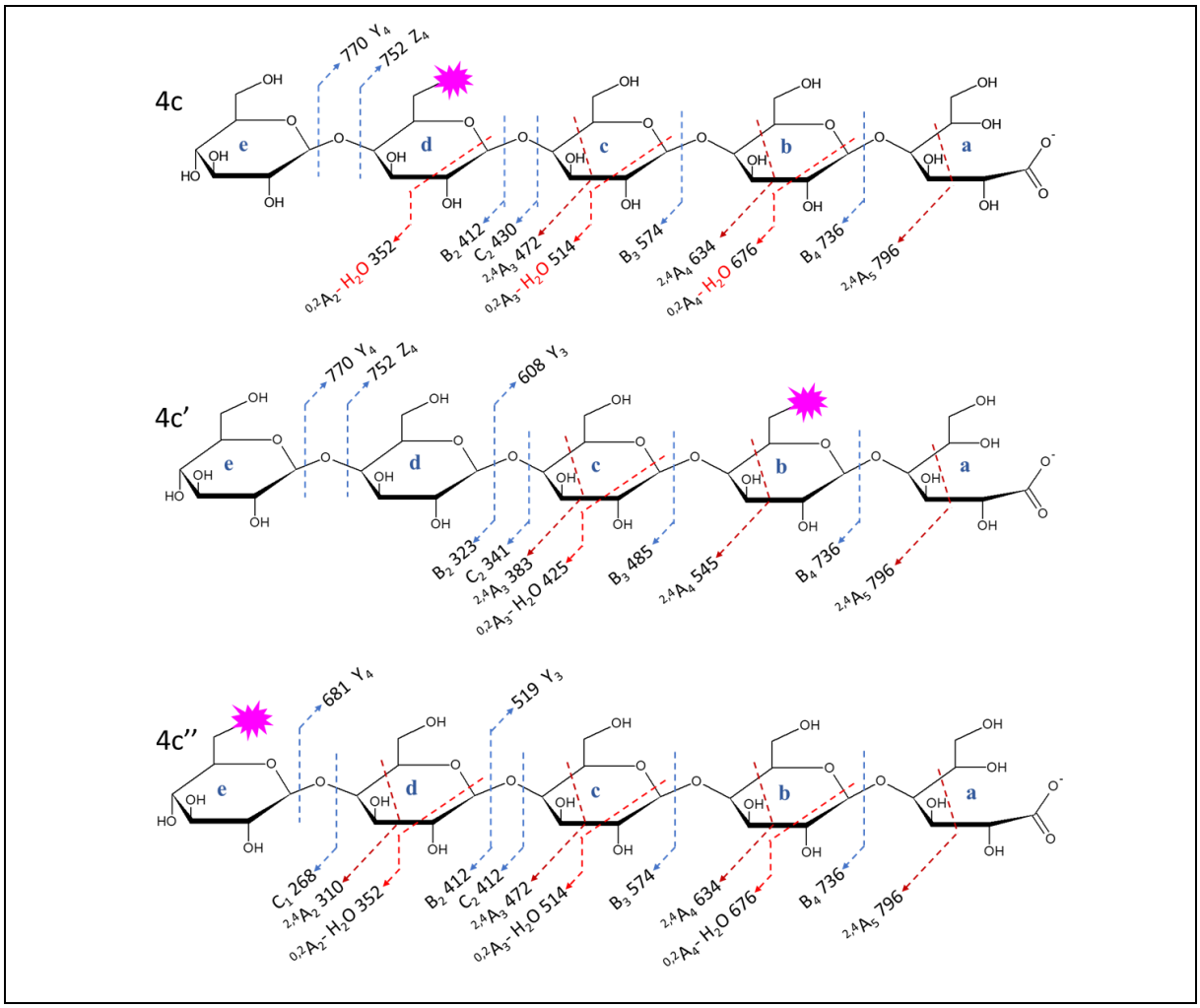

543 Fig. 6. Summary of fragmentation observed by LC-ESI-CID-MS/ MS analysis in negative ion mode of
544 products 4c, 4c' and 4c'', m/z 932.32 $[M-H]^-$. The fragments are annotated according to Domon &
545 Costello (1988).

546

547 *3.3.2 Grafting of rhodamine*

548 Encouraged by the results obtained with *p*T, we conducted the same reductive amination but with a
549 bulkier aminated molecule: the "rhodamine 123 (RHO123)". HPLC-UV-HRMS (Fig. 7) showed the
550 presence of at least 4 different products 5a-5a''', at m/z 1 169.36 ($[M-H]^-$). This mass is consistent
551 with a Glc5 molecule, on which a RHO123 molecule is grafted and that displays a carboxyl group
552 (most probably at the reducing end). Further MS/MS analysis was not performed to determine the
553 exact position of grafting.

554

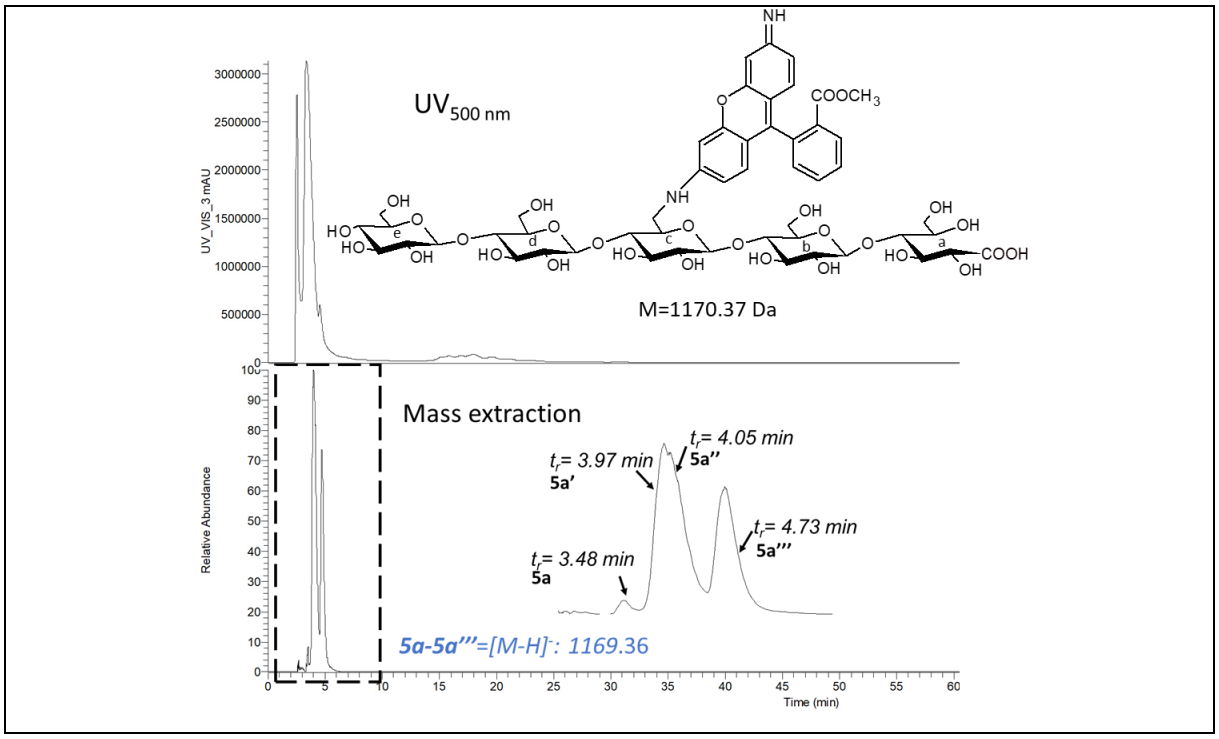

Fig. 7. LC-ESI-HRMS analysis of the glycoconjugate obtained by reductive amination of oxidized Glc5 with RHO123. $UV_{500\ nm}$ chromatogram and extracted ion chromatogram of product 5a, m/z 1 169.3. We cannot exclude that RHO123 is grafted onto the C-2 or C-3, even if these positions of grafting are less probable. The structure gives an example of a possible isomer. Reaction conditions: After 8h of enzymatic oxidation of Glc5 with TvL/TEMPO, 500 µL of the oxidized reaction medium was mixed for 3 h with 10.15 mM RHO123, 2.43 mM pic-BH_3 and 10 % acetic acid at 40°C.

3.3.3 Hydrolysis of the grafted products obtained by reductive amination

Glc5 grafted with toluidine or rhodamine was subjected to hydrolysis with a cocktail of cellulases. After reductive amination, the pH of the reaction medium was set at 4.8 and incubated with a commercial preparation of cellulases from *Trichoderma reesei* for 24 hours. HPLC-UV-HRMS analyses of the reaction mixture confirmed the presence of covalent bond between *p*T or RHO123 and Glc5 (Table S2). It is worth mentioning that we extracted a mass corresponding to a glucose molecule substituted with two toluidine molecules (m/z 359.19), which reflects the great diversity of products that can be generated (Table S2 entry 3). In the case of RHO123, the hydrolysis of the functionalized Glc5 was more difficult, resulting in the detection of non-hydrolyzed substituted DP4. It should be noted that four molecules with m/z 505.16 were identified. This mass is representative of a glucose unit substituted by one rhodamine molecule. It also proves that the substitution took place not only at the C-6 position but also at C-2, C-3 or even C-4 (when the latter is not involved in an osidic bond).

4. Conclusions

The laccase/TEMPO/O_2 system was successfully applied to the oxidation of cellobiose, methyl β-cellobiose, COS and Glc5. Oxidation of these type of oligosaccharides with LMS had never been described before. The conditions for oxidation reaction were optimized in terms of pH, temperature, time and oxygen supply for me-β-Glc2. Among the different pHs tested, the highest conversion (>70%) was obtained at pH 6, a pH value that could favour TEMPO regeneration. The introduction of both carboxyl and carbonyl groups into the COS mixture and into Glc5 was demonstrated by extensive structural analyses combining LC-MS, LC-HRMS/MS and NMR. The carbonyl groups incorporated in these oligosaccharides allowed the advantageous grafting of chromophores (*p*T and RHO123) by reductive amination. It should be noted that the combination of LMS-oxidation to reductive amination for the derivatization of oligosaccharides is effective and had never been proposed before. We showed that reductive amination can occur on different sugar units of the COS but could not define with high precision on which carbon of Glc5 glucosyl units the substituent is attached to. Only NMR or further MS studies could help clarify this point. However, the C-6 position is probably the most reactive one.

LMS-based oxidation coupled with reductive amination represents an efficient "green" route to generate negatively charged or functionalized cellooligosaccharides. The molecular diversity obtained provides access to new structures with potential prebiotic, immunostimulant, antioxidant or antitumor activities, highly sought after in the food, cosmetics and healthcare sectors. In addition, its versatility renders it applicable to different types of oligosaccharides. Although it still needs to be optimized to demonstrate its economic relevance, the proposed process is particularly attractive compared with chemical methods that require multiple protection and deprotection steps for sugar functionalization. In addition, oxidation of sugars by the laccase/Tempo system is also environmentally beneficial compared with oxidation based on TEMPO chemistry, which is generally carried out at a pH above 8 in the presence of NaOCl/NaBr and can induce cleavage between C2 and C3 of the sugar rings (Hillscher et al., 2024; Thaburet, Merbouh, Ibert, Marsais, & Queguiner, 2001). Finally, our results clearly highlight the potential of reductive amination to modify cellulose-based materials via a simple process with reduced use of hazardous or waste-generating procedures. We believe this could be of great interest to the textile industry for dyeing or modifying cotton fabrics in an eco-friendlier way.

CRediT authorship contribution statement

Awilda Maccow: Investigation, Formal analysis, visualization, Writing - Original Draft, Writing - Review & Editing. **Hanna Kulyk**: Formal analysis. **Etienne Severac**: Conceptualization, Methodology, Formal analysis, manuscript Review. **Sandrine Morel**: Conceptualization, Methodology. **Claire Moulis**: Conceptualization, Methodology, Formal analysis, manuscript Review. **Guillaume Boissonnat**: Conceptualization, Validation, Supervision, Project administration, Funding acquisition, manuscript Review. **Magali Remaud-Simeon**: Conceptualization, Methodology, Validation, Writing - Review & Editing, Visualization, Supervision, Project administration, Funding acquisition. **David Guieysse**: Conceptualization, Methodology, Validation, Investigation, Formal analysis, Writing - Review & Editing, Visualization, Supervision, Project administration, Funding acquisition.

Declaration of competing interest

The authors declare that they have no conflict of interest.

Acknowledgements

This work was funded by the National Association for Research and Technology (ANRT) and PILI company (Bioreactive projet, 2018/1179). We thank the PICT-ICEO facility dedicated to enzyme screening and discovery, and part of the Integrated Screening Platform of Toulouse (PICT, IBiSA) for providing access to equipment. PICT-ICEO is a member of IBISBA-FR (https://doi.org/10.15454/08BX-VJ91), the French node of the European research infrastructure, IBISBA (www.ibisba.eu). We thank the MetaToul-Axiom platform for giving access to the LC-HRMS facility. We are grateful to MetaToul-Fluxomet platform, the Metabolomics & Fluxomics Centre at the Toulouse Biotechnology Institute (Toulouse, France), for giving access to NMR equipment. Technical assistance provided by Valérie Bourdon from mass spectrometry platform of the ICT-UAR 2599 -(Toulouse, France - ict.cnrs.fr) is gratefully acknowledged.

Appendix A. Supplementary data

Figures S1 to S7 and Tables S1 and S2.

References

d'Acunzo, F., Galli, C., Gentili, P., & Sergi, F. (2006). Mechanistic and steric issues in the oxidation of phenolic and non-phenolic compounds by laccase or laccase-mediator systems. The case of bifunctional substrates. *New Journal of Chemistry, 30*, 583-591. https://DOI: 10.1039/b516719a

Arends, I., Li, Y.N., Ausan, R., & Sheldon, A. (2006). Comparison of TEMPO and its derivatives as mediators in laccase catalysed oxidation of alcohols. *Tetrahedron, 62*, 6659-6665. https://DOI: 10.1016/j.tet.2005.12.076

Arregui, L., Ayala, M., Gómez-Gil, X., Gutiérrez-Soto, G., Hernández-Luna, C. E., Herrera de Los Santos, M., Levin, L., Rojo-Domínguez, A., Romero-Martínez, D., Saparrat, M. C. N., Trujillo-Roldán, M. A., & Valdez-Cruz, N. A. (2019). Laccases: structure, function, and potential application in water bioremediation. *Microbial Cell Factories, 18*, 1-33. https://DOI: 10.1186/s12934-019-1248-0

Astronomo, R. D., & Burton, D. R. (2010). Carbohydrate vaccines: developing sweet solutions to sticky situations? *Nature Reviews Drug Discovery, 9*, 308-324. https://DOI:10.1038/nrd3012

Baldrian, P. (2006). Fungal laccases–occurrence and properties. *FEMS microbiology reviews, 30*, 215-242. https://DOI: 10.1111/j.1574-4976.2005.00010.x

Billès, E., Coma, V., Peruch, F., & Grelier, S. (2017). Water-soluble cellulose oligomer production by chemical and enzymatic synthesis: A mini-review. *Polymer International, 66*(9), 1227-1236. https://DOI: 10.1002/pi.5398

Cangiano, L. R., Yohe, T. T., Steele, M. A., & Renaud, D. L. (2020). Invited review: Strategic use of microbial-based probiotics and prebiotics in dairy calf rearing. *Applied Animal Science, 36*, 630-651. https://DOI: 10.15232/aas.2020-02049

Catenza, K. F., & Donkor, K. K. (2021). Recent approaches for the quantitative analysis of functional oligosaccharides used in the food industry: A review. *Food Chemistry, 355*, 129416. https://DOI: 10.1016/j.foodchem.2021.129416

Domon, B., & Costello, C.E. (1988). A systematic nomenclature for carbohydrate fragmentations in FAB-MS/MS spectra of glycoconjugates. *Glycoconjugate Journal, 5*, 397-409. https://DOI: 10.1007/BF01049915

Guo, Z., Wei, Y., Zhang, Y., Xu, Y., Zheng, L., Zhu, B., & Yao, Z. (2022). Carrageenan oligosaccharides: A comprehensive review of preparation, isolation, purification, structure, biological activities and applications. *Algal Research, 61*, 102593. https://DOI: 10.1016/j.algal.2021.102593

669 Hillscher, L.M., Höfler, M.V., Gutmann, T., Lux, C., Clerkin, K. U., Schwall, G., Villforth, K., Schabel, S.,
670 & Biesalski, M. (2024). Influence of TEMPO-oxidation on pulp fiber chemistry, morphology and
671 mechanical paper sheet properties. *Cellulose,* preprint. https://doi.org/10.1007/s10570-024-05748-5

672 Humpierre, A. R., Zanuy, A., Saenz, M., Vasco, A. V., Méndez, Y., Westermann, B., Cardoso, F.,
673 Quintero, L., Santana, D., Verez, V., Valdés, Y., Rivera, D. G., & Garrido, R. (2022). Quantitative NMR
674 for the structural analysis of novel bivalent glycoconjugates as vaccine candidates. *Journal of*
675 *Pharmaceutical and Biomedical Analysis, 214*, 114721. https://DOI: 10.1016/j.jpba.2022.114721

676 Ibrahim, O. O. (2018). Functional oligosaccharide: chemicals structure, manufacturing, health
677 benefits, applications and regulations. *Journal of Food Chemistry & Nanotechnology, 4*(4), 65-76.
678 https://DOI: 10.17756/jfcn.2018-060

679 Jaušovec, D., Vogrinčič, R., & Kokol, V. (2015). Introduction of aldehyde vs. carboxylic groups to
680 cellulose nanofibers using laccase/TEMPO mediated oxidation. *Carbohydrate Polymers, 116*, 74–85.
681 https://DOI: 10.1016/j.carbpol.2014.03.014

682 Jérôme, F., Chatel, G., & De Oliveira Vigier, K. (2016). Depolymerization of cellulose to processable
683 glucans by non-thermal technologies. *Green Chemistry, 18*, 3903-3913. https://DOI:
684 10.1039/c6gc00814c

685 Jiang, J., Ye, W., Liu, L., Wang, Z., Fan, Y., Saito, T., & Isogai, A. (2017). Cellulose nanofibers prepared
686 using the TEMPO/laccase/O_2 system. *Biomacromolecules, 18*, 288–294. https://DOI:
687 10.1021/acs.biomac.6b01682

688 Jiang, J., Chen, H., Yu, J., Liu, L., Fan, Y., Saito, T., & Isogai, A. (2021). Rate-limited reaction in
689 TEMPO/laccase/O_2 oxidation of cellulose. *Macromolecular Rapid Communications, 42*, 2000501.
690 https://DOI: 10.1002/marc.202000501

691 Jiao, L. F., Song, Z. H., Ke, Y. L., Xiao, K., Hu, C. H., & Shi, B. (2014). Cello-oligosaccharide influences
692 intestinal microflora, mucosal architecture and nutrient transport in weaned pigs. *Animal Feed*
693 *Science and Technology, 195*, 85–91. https://DOI: 10.1016/j.anifeedsci.2014.05.014

694 Kay, E., Cuccui, J., & Wren, B. W. (2019). Recent advances in the production of recombinant
695 glycoconjugate vaccines. *npj Vaccines, 4*, 1–8. https://DOI: 10.1038/s41541-019-0110-z

696 Liu, M., Liu, L., Zhang, H., Yi, B., & Everaert, N. (2021). Alginate oligosaccharides preparation,
697 biological activities and their application in livestock and poultry. *Journal of Integrative Agriculture,*
698 *20*(1), 24–34. https://DOI: 10.1016/S2095-3119(20)63195-1

699 Logtenberg, M. J., Akkerman, R., Hobé, R. G., Donners, K. M. H., Van Leeuwen, S. S., Hermes, G. D. A.,
700 de Haan, B. J., Faas, M. M., Buwalda, P. L., Zoetendal, E. G., de Vos, P., & Schols, H. A. (2021).
701 Structure-specific fermentation of galacto-oligosaccharides, isomalto-oligosaccharides and
702 isomalto/malto-polysaccharides by infant fecal microbiota and impact on dendritic cell cytokine
703 responses. *Molecular Nutrition & Food Research, 65*(16), 2001077. https://DOI:
704 10.1002/mnfr.202001077

705 Mano, M. C. R., Neri-Numa, I. A., da Silva, J. B., Paulino, B. N., Pessoa, M. G., & Pastore, G. M. (2018).
706 Oligosaccharide biotechnology: an approach of prebiotic revolution on the industry. *Applied*
707 *Microbiology and Biotechnology, 102*, 17–37. https://DOI: 10.1007/s00253-017-8564-2

708 Marzorati, M., Danieli, B., Haltrich, D., & Riva, S. (2005). Selective laccase-mediated oxidation of
709 sugars derivatives. *Green Chemistry, 7*, 310–315. https://DOI: 10.1039/B416668J

710 Mate, D.M., & Alcalde, M. (2017). Laccase: A multi-purpose biocatalyst at the forefront of
711 biotechnology. *Microbial Biotechnology, 10*, 1457–1467. https://DOI: 10.1111/1751-7915.12422

712 Morozova, O. V., Shumakovich, G. P., Shleev, S. V., & Yaropolov, Y. I. (2007). Laccase-mediator
713 systems and their applications: A review. *Applied Biochemistry and Microbiology, 43*, 523–535.
714 https://DOI: 10.1134/S0003683807050055

715 Ngo, N. T. N., Grey, C., & Adlercreutz, P. (2020a). Efficient laccase/TEMPO oxidation of alkyl
716 glycosides: effects of carbohydrate group and alkyl chain length. *Journal of Biotechnology, 324*,
717 100026. https://DOI: 10.1016/j.btecx.2020.100026

718 Ngo, N. T. N., Grey, C., & Adlercreutz, P. (2020b). Chemoenzymatic synthesis of the pH responsive
719 surfactant octyl β-D-glucopyranoside uronic acid. *Applied Microbiology and Biotechnology, 104*,
720 1055–1062. https://DOI: 10.1007/s00253-019-10254-x

721 Patel, S., & Goyal, A. (2011). Functional oligosaccharides: production, properties and applications.
722 *World Journal of Microbiology and Biotechnology, 27*, 1119–1128. https://DOI: 10.1007/s11274-010-
723 0558-5

724 Patel, I., Ludwig, R., Haltrich, D., Rosenau, T., & Potthast, A. (2011). Studies of the chemoenzymatic
725 modification of cellulosic pulps by the laccase-TEMPO system. *Holzforschung, 65*, 475–481.
726 https://DOI: 10.1515/hf.2011.035

727 Quintana, E., Roncero, M. B., Vidal, T., & Valls, C. (2017). Cellulose oxidation by Laccase-TEMPO
728 treatments. *Carbohydrate Polymers, 157*, 1488–1495. https://DOI: 10.1016/j.carbpol.2016.11.033

729 Sato, S., Sakamoto, T., Miyazawa, E., & Kikugawa, Y. (2004). One-pot reductive amination of aldehydes
730 and ketones with α-picoline-borane in methanol, in water, and in neat conditions. *Tetrahedron, 60,*
731 7899–7906. https://doi.org/10.1016/j.tet.2004.06.045

732 Schwaiger, K. N., Voit, A., Wiltschi, B., & Nidetzky, B. (2022). Engineering cascade biocatalysis in
733 whole cells for bottom-up synthesis of cello-oligosaccharides: flux control over three enzymatic steps
734 enables soluble production. *Microbial Cell Factories, 21*(61), 1-14. https://DOI: 10.1186/s12934-022-
735 01781-w

736 Solomon, E.I., Sundaram, U. M., & Machonkin, T. E. (1996). Multicopper oxidases and oxygenases.
737 *Chemical Reviews, 96*, 2563–2606. https://DOI: 10.1021/cr950046o

738 Sun, P., Frommhagen, M., Haar, M. K., van Erven, G., Bakx, E. J., van Berkel, W. J. H., & Kabel, M. A.
739 (2020). Mass spectrometric fragmentation patterns discriminate C1- and C4-oxidised cello-
740 oligosaccharides from their non-oxidised and reduced forms. *Carbohydrate Polymers, 234*, 115917.
741 https://DOI: 10.1016/j.carbpol.2020.115917

742 Thaburet, J.-F., Merbouh, N., Ibert, M., Marsais, F., & Queguiner, G. (2001). TEMPO-mediated
743 oxidation of maltodextrins and d-glucose: effect of pH on the selectivity and sequestering ability of
744 the resulting polycarboxylates. *Carbohydrate Research, 330*, 21–29. https://doi.org/10.1016/S0008-
745 6215(00)00263-9

746 Theerachat, M., Guieysse, D., Morel, S., Remaud-Simeon, M., & Chulalaksananukul, W. (2019).
747 Laccases from marine organisms and their applications in the biodegradation of toxic and
748 environmental pollutants: A review. *Applied Biochemistry and Biotechnology, 187*, 583–611.
749 https://DOI: 10.1007/s12010-018-2829-9

750 Uyeno, Y., Shigemori, S., & Shimosato, T. (2015). Effect of probiotics/prebiotics on cattle health and
751 productivity. *Microbes and Environments, 30*, 126–132. https://DOI: 10.1264/jsme2.ME14176

752 Vasudevan, U. M., Lee, O. K., & Lee, E. Y. (2021). Alginate derived functional oligosaccharides: Recent
753 developments, barriers, and future outlooks. *Carbohydrate Polymers, 267*, 118158. https://DOI:
754 10.1016/j.carbpol.2021.118158

755 Vuong, T. V., Vesterinen, A.-H., Foumani, M., Juvonen, M., Seppälä, J., Tenkanen, M., & Master, E. R.
756 (2013). Xylo- and cello-oligosaccharide oxidation by gluco-oligosaccharide oxidase from *Sarocladium*
757 *strictum* and variants with reduced substrate inhibition. *Biotechnology for Biofuels, 6*, 148.
758 https://DOI: 10.1186/1754-6834-6-148

759 Westereng, B., Kračun, S. K., Leivers, S., Arntzen, M. Ø., Aachmann, F. L., & Eijsink, V. G. H. (2020).
760 Synthesis of glycoconjugates utilizing the regioselectivity of a lytic polysaccharide monooxygenase.
761 *Scientific Reports, 10*, 13197. https://DOI: 10.1038/s41598-020-69951-7

762 Yamasaki, N., Ibuki, I., Yaginuma, Y., & Tamura, Y. (2013). Cellooligosaccharide-containing
763 composition. US8349365B2.

764 Yoshida, H. (1883). Chemistry of lacquer (Urushi). Part I. Communication from the chemical society of
765 Tokyo. *Journal of the Chemical Society, Transactions, 43*, 472–486. https://DOI:
766 10.1039/CT8834300472

767 Yu, Y., Wang, Q., Yuan, J., Fan, X., & Wang, P. (2016). A novel approach for grafting of β-cyclodextrin
768 onto wool via laccase/TEMPO oxidation. *Carbohydrate Polymers, 153*, 463–470. https://DOI:
769 10.1016/j.carbpol.2016.08.003

770 Zhang, Y.-H.P., & Lynd, L. R. (2003). Cellodextrin preparation by mixed-acid hydrolysis and
771 chromatographic separation. *Analytical Biochemistry, 322*, 225–232. https://DOI:
772 10.1016/j.ab.2003.07.021

773 Zhong, C., Ukowitz, C., Domig, K. J., & Nidetzky, B. (2020). Short-chain cello-oligosaccharides:
774 intensification and scale-up of their enzymatic production and selective growth promotion among
775 probiotic bacteria. *Journal of Agricultural and Food Chemistry, 68*, 8557–8567. https://DOI:
776 10.1021/acs.jafc.0c02660

777

778